

# A comparative metabolomic analysis reveals the metabolic variations among cartilage of Kashin-Beck disease and osteoarthritis

From Xi'an Jiaotong University,  
Xi'an, China

H. Chang,<sup>1</sup> L. Liu,<sup>2</sup> Q. Zhang,<sup>1</sup> G. Xu,<sup>1</sup> J. Wang,<sup>3</sup> P. Chen,<sup>1</sup> C. Li,<sup>1</sup> X. Guo,<sup>1</sup> Z. Yang,<sup>1</sup> F. Zhang<sup>2</sup>

<sup>1</sup>Shaanxi Provincial Institute for Endemic Disease Control, Xi'an, China

<sup>2</sup>School of Public Health, Health Science Center, Xi'an Jiaotong University, Xi'an, China

<sup>3</sup>Department of Joint Surgery, Honghui Hospital, Xi'an Jiaotong University, Xi'an, China

Cite this article:

*Bone Joint Res* 2024;13(7):  
362–371.

DOI: 10.1302/2046-3758.  
137.BJR-2023-0403.R1

Correspondence should be  
sent to Zhengjun Yang  
[382747669@qq.com](mailto:382747669@qq.com)

## Aims

The metabolic variations between the cartilage of osteoarthritis (OA) and Kashin-Beck disease (KBD) remain largely unknown. Our study aimed to address this by conducting a comparative analysis of the metabolic profiles present in the cartilage of KBD and OA.

## Methods

Cartilage samples from patients with KBD (n = 10) and patients with OA (n = 10) were collected during total knee arthroplasty surgery. An untargeted metabolomics approach using liquid chromatography coupled with mass spectrometry (LC-MS) was conducted to investigate the metabolomics profiles of KBD and OA. LC-MS raw data files were converted into mzXML format and then processed by the XCMS, CAMERA, and metaX toolbox implemented with R software. The online Kyoto Encyclopedia of Genes and Genomes (KEGG) database was used to annotate the metabolites by matching the exact molecular mass data of samples with those from the database.

## Results

A total of 807 ion features were identified for KBD and OA, including 577 positive (240 for upregulated and 337 for downregulated) and 230 negative (107 for upregulated and 123 for downregulated) ions. After annotation, LC-MS identified significant expressions of ten upregulated and eight downregulated second-level metabolites, and 183 upregulated and 162 downregulated first-level metabolites between KBD and OA. We identified differentially expressed second-level metabolites that are highly associated with cartilage damage, including dimethyl sulfoxide, uric acid, and betaine. These metabolites exist in sulphur metabolism, purine metabolism, and glycine, serine, and threonine metabolism.

## Conclusion

This comprehensive comparative analysis of metabolism in OA and KBD cartilage provides new evidence of differences in the pathogenetic mechanisms underlying cartilage damage in these two conditions.

## Article focus

- The variance in articular damage between osteoarthritis (OA) and Kashin-Beck disease (KBD).
- The contrast in metabolic changes of cartilage between OA and KBD.
- Key metabolites and enriched pathways involved in the pathogenesis of KBD.

## Key messages

- Ten upregulated and eight downregulated second-level metabolites were identified for KBD compared to OA.
- The level of uric acid in the cartilage of KBD was increased compared to OA.
- Purine metabolism is involved in the cartilage metabolism of KBD.

## Strengths and limitations

- This is the first study to compare the metabolic profiling of cartilage between OA and KBD.
- This finding highlights the distinct pathophysiological mechanisms underlying these two conditions.
- The articular samples included are relatively limited. Further validation studies are warranted in a larger sample.
- The alterations in metabolites present in the blood, urine, and synovial fluid samples of patients with OA and KBD should be identified and compared with the metabolic findings in cartilage tissue.

## Introduction

Kashin-Beck disease (KBD) is a serious, endemic chronic osteochondral disease that was first reported in 1849. The high prevalence of KBD mainly occurs in agricultural regions in southeastern Siberia and China,<sup>1</sup> affecting approximately two million people in northern China. KBD is characterized by multiple symptoms affecting growth and articular cartilage, including symmetrical enlargement of the phalanges, brachydactyly, joint deformity, and even dwarfism. The main feature of KBD is its short stature, which is caused by several focal necroses in the growth plate, leading to secondary osteoarthritis (OA). Although much effort has been made, the specific mechanisms underlying KBD remain unclear. Previous studies have identified several risk factors for KBD, including environmental selenium deficiency,<sup>1</sup> dietary fungal toxin contaminations,<sup>2</sup> and water-organic compound poisoning. In addition, experiments have revealed multiple processes involved in cartilage damage in KBD, such as apoptosis,<sup>3</sup> extracellular matrix (ECM) degradation,<sup>4</sup> metabolism,<sup>5</sup> and inflammation.<sup>6</sup> In addition to environmental factors, family and epidemiological studies indicate that genetic variants have a key role in modifying the disease course. It has been estimated that the heritability of KBD ranges from 35.10% to 41.76% in families, indicating that genetic factors play an important role in the development of KBD.<sup>7</sup> A previous study suggested that genetic factors may be more important than selenium deficiency in the pathogenesis of KBD, indicating that KBD is a complex disease caused by the interaction of multiple genes and environmental factors.<sup>8</sup>

OA is a chronic, progressive degenerative joint disease of middle-aged and elderly people, contributing to a higher burden of disease in China and the world.<sup>9</sup> OA commonly affects the hands, hips, knees, and spine, causing pain, stiffness, and swelling in the affected joints. Researchers have made an effort to understand the risk factors associated with cartilage damage<sup>10</sup> and diagnostic biomarkers for OA,<sup>11</sup> however the underlying mechanisms remain unclear. As with KBD, OA pathogenesis is considered to be a multifactorial polygenic disease,<sup>12</sup> involving interactions between genes and the environment, and environmental changes are major contributors to the current high prevalence of OA. KBD is an endemic and degenerative form of OA, and is similar in clinical manifestation and several aspects of its pathological features, including ECM degradation, cartilage lesions, and reduction and destruction of proteoglycans and collagen. In addition, it was found that the prevalence of hand OA was closely related to the pathogenic factors of KBD.<sup>13</sup> However, the aetiology of KBD sets it apart from OA,

despite their similar pathological outcomes. Previous studies have also discussed the differences in the aetiology and molecular mechanism between KBD and OA. For example, the cartilage damage of KBD mainly manifests as a focal chondronecrosis of the deep zone and ECM degradation of both growth plate cartilage and articular cartilage,<sup>2</sup> while OA was mainly manifested as progressive degradation in the superficial zone and synovial inflammation.<sup>14</sup> In addition, KBD tends to occur in the growth period of children and adolescents, however OA is a degenerative disease that progresses with ageing. A gene set enrichment analysis (GSEA) was conducted to identify differentially expressed genes and pathways between OA and KBD, and found that the apoptosis- and nitric oxide (NO)-related pathways were significantly upregulated in the KBD cartilage, while the reactive oxygen species (ROS)- and vascular endothelial growth factor A (VEGF-A)-related pathways were significantly upregulated in the OA cartilage, indicating the difference of pathology mechanisms between KBD and OA.<sup>15</sup> The differences in the microbiome between KBD and OA were also confirmed using 16S rDNA gene sequencing and metagenomic sequencing.<sup>16</sup> Thus, given the high correlation between these two disorders, it is important to comprehensively compare the differences and similarities in their pathology, and clarify the underlying mechanisms for KBD.

Metabolomics is the profiling of metabolites in biofluids, cells, and tissues. Given the high sensitivity of metabolomics in detecting subtle alterations in biological pathways, metabolomics has been routinely applied as a tool for biomarker discovery, thus providing insight into the mechanisms underlying complex diseases.<sup>17</sup> In addition, evidence is emerging for a key role for metabolism in cartilage and synovial joint function. According to previous studies, a variety of pathophysiological events seen in KBD are related to metabolic changes. Wang et al<sup>5</sup> performed a serum metabolomic analysis and identified disordered lipid metabolism metabolic networks involved in the pathogenesis of KBD. Another two-stage metabolomic study demonstrated that sphingolipid metabolic pathways may be closely related to KBD.<sup>18</sup> OA is a metabolic disorder, and the dysregulated metabolism in chondrocytes of OA has also been identified.<sup>19</sup> Metabolism has a key role in the physiological turnover of synovial joint tissues, including articular cartilage.<sup>20</sup> A systematic review was conducted to identify metabolites in published literature in human synovial fluid, and found over 200 metabolites. Among them, 26 putative biomarkers have been demonstrated in OA, inflammatory arthropathies, and trauma.<sup>21</sup> However, the difference concerning the metabolic alterations in articular cartilage of KBD and OA has not been well studied.

In the current study, we performed untargeted mass spectrometry-based metabolomics and investigated the different metabolic pathways in the articular cartilage of KBD and OA patients. Our study aimed to facilitate a critical understanding of the metabolic alterations in comparisons of KBD and OA, and provide a novel perspective on the management and treatment of KBD.

**Table 1.** Basic characteristics of study subjects.

Subjects	Mean age, yrs (SD)	Female, n (%)
KBD (n = 10)	64.6 (4.93)	8 (80)
OA (n = 10)	69.6 (9.83)	3 (30)

KBD, Kashin-Beck disease; OA, osteoarthritis; SD, standard deviation.

## Methods

### Study population

A total of ten OA patients and ten KBD patients were included in the present study. Clinical specimens of articular cartilage were harvested from patients undergoing primary total knee arthroplasty. KBD patients were diagnosed strictly according to the national diagnostic criteria of KBD in China (WS/T 207-2010), and OA patients were diagnosed strictly according to the Modified Outerbridge Classification.<sup>22</sup> Patients were diagnosed with KBD based on the radiograph alterations, including defects and sclerosis on the bone end of phalanges combined with compression changes of the calcaneus and talus, and enlarged/deformed limb joints (hand, elbow, knee, ankle, etc). Both KBD and OA patients were excluded for the following reasons: they were suffering or had previously suffered from any other osteoarticular diseases (such as rheumatoid arthritis, gout, or skeletal fluorosis) or any other type of macrosomia, osteochondrodysplasia, or chronic disease (such as hypertension, diabetes, or coronary heart disease). All recruited patients with Kashin-Beck disease and osteoarthritis were local residents of Shaanxi province with similar eating habits. All study subjects were Chinese Han and matched for sex. For each participant, a written informed consent form and their general clinical data were obtained, including self-reported ethnicity, age, sex, educational background, BMI, health status, and medical histories. Based on the inclusion and exclusion criteria, there were ten patients with KBD and ten patients with OA included in the study.

### Untargeted metabolite profiling of KBD and OA cartilage

An untargeted metabolomic approach was performed to explore the difference in chondrocyte metabolic profiling involved in the pathogenesis of KBD and OA. A total of ten patients with KBD and ten patients with OA were recruited. The collected knee cartilage samples of KBD (Figure 1a) and OA (Figure 1b) are displayed in Figure 1. The demographic characteristics of the two groups are summarized in Table 1. The quality control for features obtained by XCMS software was conducted by the overall MS signal intensity controlled by total ion chromatogram (TIC), evaluation of width for m/z peak, and assessment of width for RT peak for each feature. The TIC results showed a high degree of overlap (Supplementary Figures a and b). In addition, the m/z width and retention-time width analyses suggested that the sample preparation and instrument state met the required standards (Supplementary Figures c and d). After peak alignment, peak extraction, and peak area calculations, 5,574 positive-mode features and 8,568 negative-mode features were detected in KBD and OA subjects. An overview of the metabolite profiling of KBD and OA is shown in Figure 1c.

### Cartilage explant harvest and sample preparation

Cartilage explants were harvested<sup>23</sup> and sample preparation<sup>24</sup> was conducted as follows. All articular cartilage samples were harvested from the lateral tibial plateau and obtained within one hour after operation. Samples were then transported immediately to the laboratory, cut into pieces (1 mm), divided into three portions per sample, packed into freezer tubes, frozen in liquid nitrogen overnight, and preserved at -80°C for further metabolic profiling analysis. The collected samples were thawed on ice, and metabolites were extracted with 50% methanol buffer. Briefly, 100 mg of cartilage was extracted with 120 µl of precooled 50% methanol, vortexed, and incubated at room temperature for ten minutes; the extraction mixture was then stored overnight at -20°C. After centrifugation at 4,000× g for 20 minutes, the supernatants were transferred into new 96-well plates. Pooled quality control samples were prepared by combining 10 µl of each extraction mixture. The samples were stored at -80°C prior to liquid chromatography coupled with mass spectrometry (LC-MS) analysis.

### LC-MS analysis

All samples were acquired by the LC-MS system following machine orders.<sup>24,25</sup> Firstly, all chromatographic separations were performed using a Thermo Scientific UltiMate 3000 HPLC. An ACQUITY UPLC BEH C18 column (100 mm\*2.1 mm, 1.8 µm; Waters, UK) was used for the reversed phase separation. The column oven was maintained at 35°C. The flow rate was 0.4 ml/min and the mobile phase consisted of solvent A (water, 0.1% formic acid) and solvent B (Acetonitrile, 0.1% formic acid). Gradient elution conditions were set as follows: 0 to 0.5 minutes, 5% B; 0.5 to 7 minutes, 5% to 100% B; 7 to 8 minutes, 100% B; 8 to 8.1 minutes, 100% to 5% B; and 8.1 to 10 minutes, 5%B. The injection volume for each sample was 4 µl.<sup>26</sup>

A high-resolution tandem mass spectrometer Q-Exactive (Thermo Fisher Scientific, USA) was used to detect metabolites eluted from the column. The Q-Exactive was operated in both positive and negative ion modes. Precursor spectra (70-1050 mass-to-charge ratio (m/z)) were collected at 70,000 resolutions to hit an automatic gain control (AGC) target of 3e6. The maximum injection time was set to 100 ms. A top three configuration to acquire data was set in data-dependent acquisition (DDA) mode. Fragment spectra were collected at 17,500 resolutions to hit an AGC target of 1e5 with a maximum injection time of 80 ms. To evaluate the stability of the LC-MS during the whole acquisition, a quality control sample (pool of all samples) was acquired after every ten samples.

### Bioinformatic analysis of the untargeted metabolomic dataset

The acquired MS data pre-treatments, including peak picking, peak grouping, retention time (RT) correction, second peak grouping, and annotation of isotopes and adducts, were performed using XCMS software (Siuzdak Lab, USA). LC-MS raw data files were converted into mzXML format and then processed by the XCMS, CAMERA, and metaX toolbox implemented with R software (R Foundation for Statistical Computing, Austria).<sup>27-29</sup> XCMS (an acronym for various forms (X) of chromatography mass spectrometry, XCMS)<sup>27</sup> is a LC/

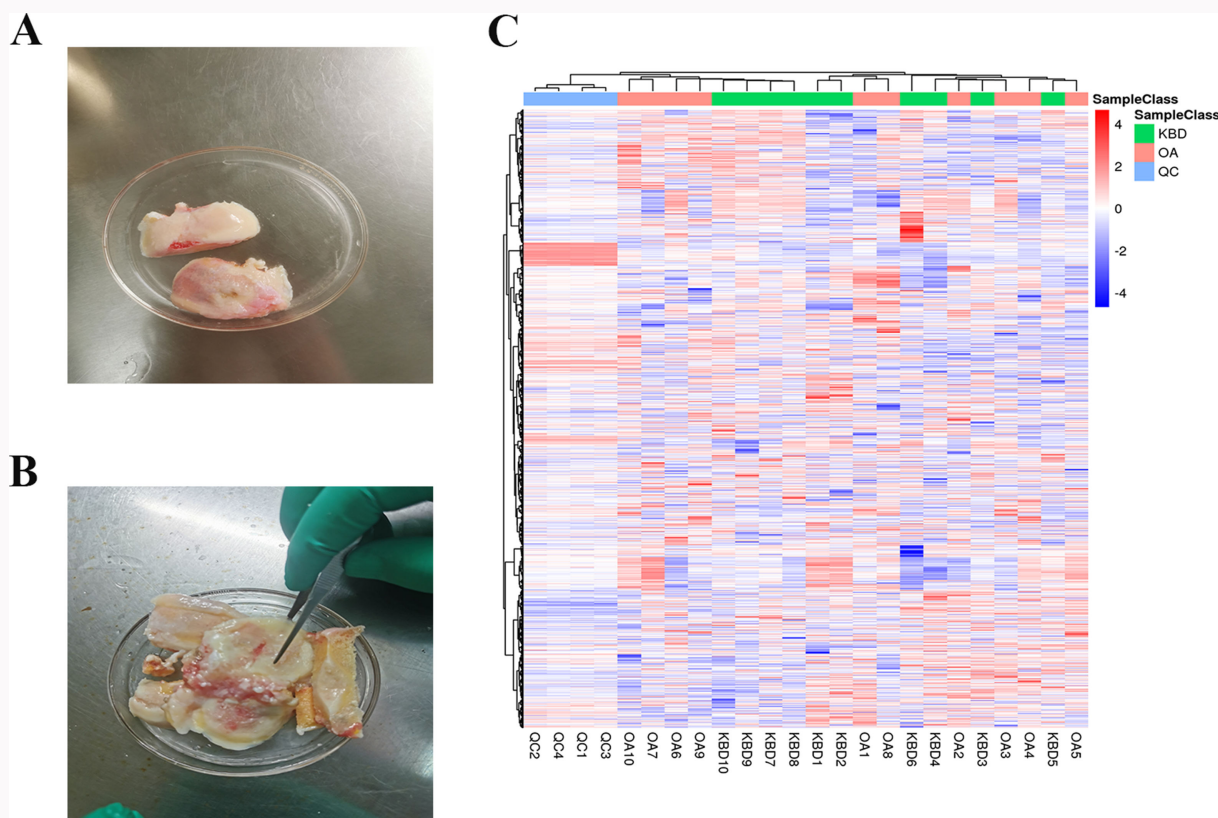


**Fig. 1** The basic characteristics of study subjects with Kashin-Beck disease (KBD) and osteoarthritis (OA). a) and b) The cartilage specimens were derived from the patients with a) KBD and b) OA. c) The heatmap of all changed features in KBD and OA. QC, quality control.

MS-based data analysis approach, which incorporates novel nonlinear RT alignment, matched filtration, peak detection, and peak matching. CAMERA (Collection of Algorithms for MEtabolite pRofile Annotation)<sup>28</sup> is a bioconductor package integrating algorithms to extract compound spectra, annotate isotope and adduct peaks, and propose accurate compound mass even in highly complex data. metaX<sup>29</sup> is an R package, which is easy to use for the analysis of metabolomics data generated from mass spectrometry. Each ion was identified by combining RT and *m/z* data. Intensities of each peak were recorded, and a 3D matrix containing arbitrarily assigned peak indices (RT-*m/z* pairs), sample names (observations), and ion intensity information (variables) was generated.

The online Kyoto Encyclopedia of Genes and Genomes (KEGG) database<sup>30</sup> was used to annotate the metabolites by matching the exact molecular mass data (*m/z*) of samples with those from the database. If a mass difference between the observed and the database value was less than 10 ppm, the metabolite would be annotated and the molecular formula of metabolites would further be identified and validated by the isotopic distribution measurements. We also used an in-house fragment spectrum library of metabolites to validate the metabolite identification.<sup>24</sup>

The intensity of peak data was further preprocessed by metaX. Those features detected in less than 50% of quality control samples or 80% of biological samples were removed, and the remaining peaks with missing values were imputed with the *k*-nearest neighbor algorithm to further improve the data quality. PCA was performed for outlier

detection and batch effects evaluation using the pre-processed dataset. Quality control-based robust locally estimated scatterplot smoothing (LOESS) signal correction was fitted to the quality control data concerning the order of injection to minimize signal intensity drift over time. In addition, the relative standard deviations of the metabolic features were calculated across all quality control samples, and those > 30% were then removed.

### Statistical analysis

For the untargeted metabolomic analysis, independent-samples *t*-tests were conducted to detect differences in metabolite concentrations between two phenotypes. Supervised partial least squares discriminant analysis (PLS-DA) was conducted through metaX to discriminate the different variables between groups. The variable importance in projection (VIP) value was calculated and used to select important features. Metabolites with VIP values  $\geq 1.0$ , fold change (FC)  $\geq 1.2$  or  $\leq 0.83$ , and *p*-values < 0.05 were considered to be potential differential metabolites.

### Results

#### Differentially expressed metabolites between KBD and OA cartilage

The PLS-DA model was applied to determine the profile of discriminant metabolites in KBD and OA cartilage (Figures 2a and 2b). The PLS-DA uses partial least squares regression to establish the relationship model between metabolite expression and a sample class. The goodness of fit parameter

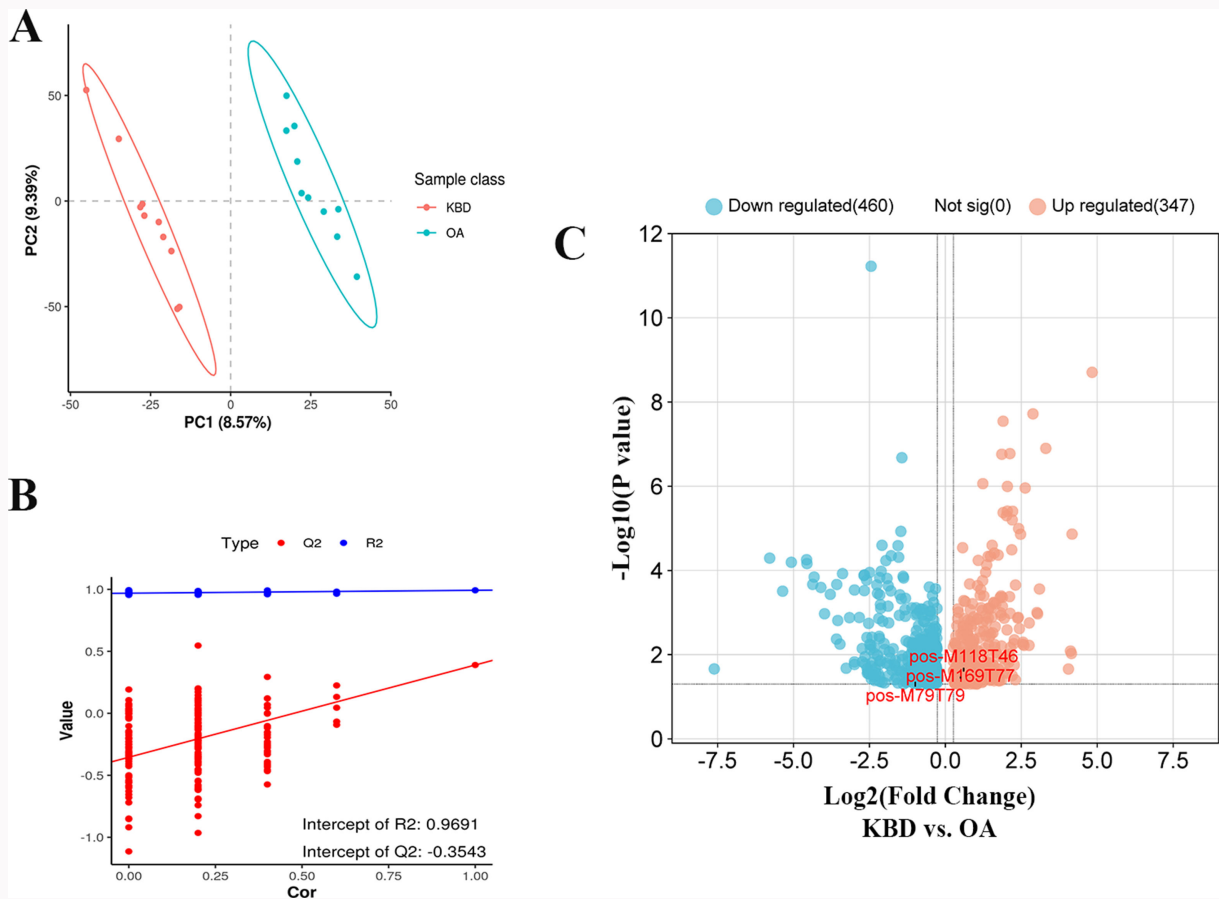


**Fig. 2**

Significantly changed molecular features between Kashin-Beck disease (KBD) and osteoarthritis (OA). a) Score plots of partial least squares discriminant analysis (PLS-DA) of the positive and negative modes from KBD patients and OA patients. b) Validation plot for PLS-DA model. The Y-axis intercepts were  $R^2$  (0.0, 0.9691) and  $Q^2$  (0.0, -0.3543). The criteria for stability and credibility are as follows: all permuted  $R^2$  and  $Q^2$  values on the left-bottom corner are lower than the associated initial values (top-right corner), and the  $Q^2$  regression line in red has a negative intercept. c) The volcano plot of 807 negative and positive detected features between KBD and OA patients. All p-values in c) were calculated using independent-samples t-test. Cor, correlation coefficient.

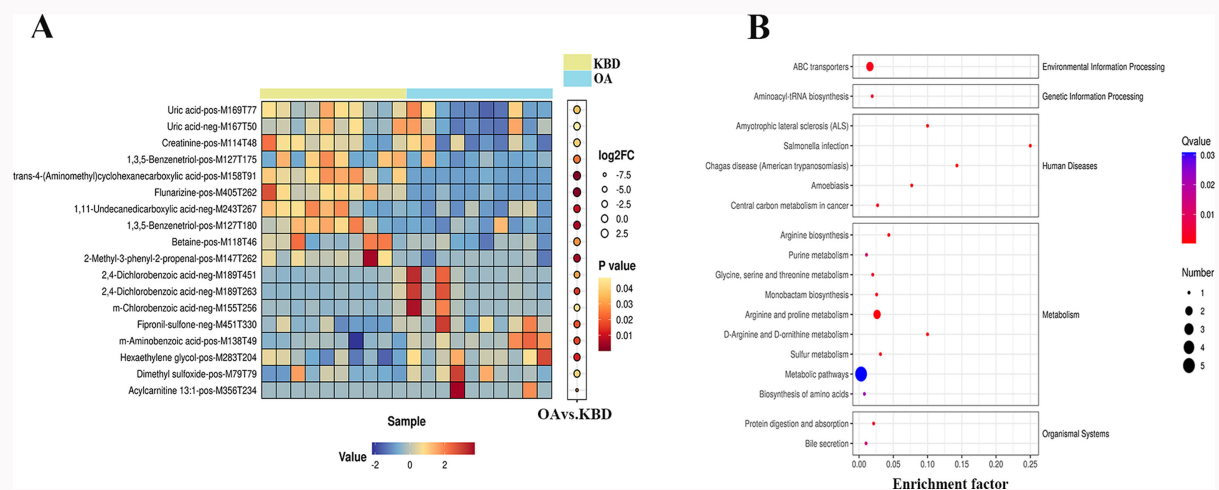


**Fig. 3**

Classification of differential metabolites and pathways enriched between Kashin-Beck disease (KBD) and osteoarthritis (OA). a) Heat map of 18 differentially accumulating second-level metabolite cluster analyses between KBD and OA. Differential metabolites were defined as metabolites with fold change  $\geq 1.2$  or  $\leq 0.83$  in KBD compared with OA. A threshold of variable importance in projection (VIP)  $> 1.0$  was used to separate differential metabolites from non-significantly differential metabolites. b) Kyoto Encyclopedia of Genes and Genomes (KEGG) enrichment bubble plot of second-level metabolites. All p-values in a) were calculated using independent-samples t-test.

**Table II.** Identification of the second-level differential metabolites related to the pathogenesis of Kashin-Beck disease.

ID	m/z	RT	Metabolites	FC	p-value*	VIP
neg-M167T50	167.0207	0.8329	Uric acid	1.4182	0.047	1.9399
pos-M169T77	169.0353	1.2842	Uric acid	1.4080	0.036	1.9299
pos-M158T91	158.1173	1.5084	trans-4-(Aminomethyl)cyclohexanecarboxylic acid	9.8959	< 0.001	5.5213
neg-M155T256	154.9903	4.2733	m-Chlorobenzoic acid	0.2225	0.043	2.5826
pos-M138T49	138.0536	0.8179	m-Aminobenzoic acid	0.6427	0.016	1.9632
pos-M283T204	283.1746	3.3943	Hexaethylene glycol	0.8026	0.012	1.1129
pos-M405T262	405.2131	4.3675	Flunarizine	18.0192	< 0.001	7.7590
neg-M451T330	450.9264	5.5062	Fipronil-sulfone	0.5055	0.018	2.2582
pos-M79T79	79.0178	1.3249	Dimethyl sulfoxide	0.5034	0.040	3.0479
pos-M114T48	114.0659	0.8000	Creatinine	1.5784	0.039	2.2151
pos-M118T46	118.0860	0.7659	Betaine	1.5177	0.028	1.7352
pos-M356T234	356.2787	3.8998	Acylcarnitine 13:1	0.0051	0.022	4.0802
pos-M147T262	147.0802	4.3587	2-Methyl-3-phenyl-2-propenal	1.8193	0.005	2.2832
neg-M189T451	188.9512	7.5164	2,4-Dichlorobenzoic acid	0.1918	0.030	3.0699
neg-M189T263	188.9513	4.3797	2,4-Dichlorobenzoic acid	0.1503	0.015	3.7835
pos-M127T175	127.0500	2.9248	1,3,5-Benzenetriol	2.6124	0.024	2.7787
pos-M127T180	127.0388	3.0043	1,3,5-Benzenetriol	2.6864	0.006	3.2320
neg-M243T267	243.1600	4.4428	1,11-Undecanedicarboxylic acid	1.3140	0.009	1.4955

\*Independent-samples *t*-test.

FC, fold change; m/z, mass-to-charge ratio; RT, retention time; VIP, variable importance in projection.

( $R^2$ ) and predictive power parameter ( $Q^2$ ) values were used to evaluate the quality of our model.  $R^2$  indicates the interpretation rate of the built model to the X and Y matrix, while  $Q^2$  reflects the proportion of variance in the data predicted by the model, which translates into the model's prediction ability. The ion model with  $R^2$  and  $Q^2$  mean values were 0.9691 and -0.3543, indicating that the current PLS-DA model is more reliable (Figure 2b). The metabolic variances in cartilage between KBD and OA were examined through LC-MS analysis. A total of 807 ion features (Figure 2c) were detected in KBD and OA, which consisted of 577 positive ions (240 upregulated and 337 downregulated) and 230 negative ions (107 upregulated and 123 downregulated). After annotation, we detected ten second-level metabolites that were upregulated and eight that were downregulated (Table II). Additionally, it revealed 183 upregulated and 162 downregulated first-level metabolites. The cluster heatmap plot of the differential second-level metabolites enriched in KBD versus OA samples is presented in Figure 3a, in which colour intensity correlates with the degree of increase (red) and decrease (blue) relative to the mean metabolite ratio. The identified differentially expressed second-level metabolites, which are highly associated with cartilage damage, include dimethyl sulfoxide (DMSO), uric acid, and betaine.

#### Differentially involved pathways between KBD and OA cartilage

In addition, all the differential second-level metabolites in the KBD and OA comparison groups were matched to the

KEGG database to obtain the metabolic pathway information. KEGG annotation and enrichment analysis were conducted, and the enriched pathways are shown in Figure 3b and Table III. For OA versus KBD, the enriched pathways of differential metabolites contained purine metabolism, sulphur metabolism, and metabolic pathways.

#### Discussion

Previous studies have attempted to evaluate the metabolite profile using various KBD models, including urinary samples from KBD children,<sup>31</sup> gut microbiota from KBD patients,<sup>5</sup> and serum samples from KBD patients.<sup>32</sup> These studies have revealed a notable discovery that metabolic changes coexist with the progression of KBD. However, very few studies have compared the cartilage metabolic profiling of OA and KBD.<sup>33,34</sup> In the present study, we conducted an untargeted metabolomic profiling of KBD and OA cartilage and identified a group of differentially second-level metabolites and enriched pathways for KBD. To the best of our knowledge, this is the first study to explore the roles of metabolites in the comparison of KBD and OA. Our results indicate the implication of metabolite profiling alterations in the development of KBD, and provide clues on the therapeutic targets for KBD in clinical practice.

Metabolites are generally viewed as intermediates or products of metabolism. Due to their direct involvement in biochemical activity markers, metabolites tend to reflect phenotypic relationships. Bone and joint tissues exhibit high metabolic activity, and it continuously undergoes remodelling to maintain its equilibrium. This remodelling process results in

**Table III.** Identification of significantly abnormally expressed pathways related for Kashin-Beck disease and osteoarthritis patients.

Level 1	Level 2	Pathway	Pathway ID	Compound	Feature	p-value*
Environmental information processing	Membrane transport	ABC transporters	map02010	L-Arginine; betaine	pos-M175T44; pos-M118T46	0.001
Genetic information processing	Translation	Aminoacyl-tRNA biosynthesis	map00970	L-Arginine	pos-M175T44	0.004
Human diseases	Cancers: Overview	Central carbon metabolism in cancer	map05230	L-Arginine	pos-M175T44	0.002
Human diseases	Infectious diseases: Bacterial	<i>Salmonella</i> infection	map05132	L-Arginine	pos-M175T44	< 0.001
Human diseases	Infectious diseases: Parasitic	Amoebiasis	map05146	L-Arginine	pos-M175T44	< 0.001
Human diseases	Infectious diseases: Parasitic	Chagas disease (American trypanosomiasis)	map05142	L-Arginine	pos-M175T44	< 0.001
Human diseases	Neurodegenerative diseases	Amyotrophic lateral sclerosis (ALS)	map05014	L-Arginine	pos-M175T44	< 0.001
Metabolism	Amino acid metabolism	Arginine and proline metabolism	map00330	L-Arginine; creatinine	pos-M175T44; pos-M114T48	< 0.001
Metabolism	Amino acid metabolism	Arginine biosynthesis	map00220	L-Arginine	pos-M175T44	< 0.001
Metabolism	Amino acid metabolism	Glycine, serine, and threonine metabolism	map00260	Betaine	pos-M118T46	0.003
Metabolism	Biosynthesis of other secondary metabolites	Monobactam biosynthesis	map00261	L-Arginine	pos-M175T44	0.002
Metabolism	Energy metabolism	Sulphur metabolism	map00920	Dimethyl sulfoxide	pos-M79T79	0.001
Metabolism	Global and overview maps	Metabolic pathways	map01100	L-Arginine; Urate; Betaine; Creatinine; 2,4-Dichlorobenzoate	pos-M175T44; neg-M167T50; pos-M169T77; pos-M118T46; pos-M114T48; neg-M189T263; neg-M189T451	0.031
Metabolism	Global and overview maps	Biosynthesis of amino acids	map01230	L-Arginine	pos-M175T44	0.021
Metabolism	Metabolism of other amino acids	D-Arginine and D-ornithine metabolism	map00472	L-Arginine	pos-M175T44	< 0.001
Metabolism	Nucleotide metabolism	Purine metabolism	map00230	Urate	neg-M167T50; pos-M169T77	0.011
Organismal systems	Digestive system	Bile secretion	map04976	Urate	neg-M167T50; pos-M169T77	0.013
Organismal systems	Digestive system	Protein digestion and absorption	map04974	L-Arginine	pos-M175T44	0.003

\*Independent-samples *t*-test.

KBD, Kashin-Beck disease; OA, osteoarthritis.

alterations in several metabolites, which can act as diagnostic indicators for bone and joint disorders. For example, lipid metabolism and lipid metabolites were found to influence different features of cartilage, and affect the cartilage growth, degeneration, and regeneration processes in diverse ways.<sup>35</sup> Long-chain polyunsaturated fatty acids (LCPUFAs) and their metabolites are considered to be essential

factors in supporting bone and joint health.<sup>36</sup>  $\alpha$ -KG is an essential physiological metabolite from the mitochondrial tricarboxylic acid (TCA) cycle, and  $\alpha$ -KG supplementation could alleviate osteoarthritic phenotype by regulating mitophagy and oxidative stress, suggesting its potential as a therapeutic target to ameliorate OA.<sup>37</sup> Taken together, the evidence above

suggests the important therapeutic role of metabolites in the progression of bone and joint disease.

Several differential metabolites were identified in the cartilage of KBD and OA. An important finding from the present study was that the DMSO was downregulated in KBD compared to OA. DMSO is not a compound that naturally exists in the human body; it is likely an exogenous 'contaminant' as it is widely used as a solvent in many pharmaceuticals. DMSO can be exposed to the human body in a variety of ways due to its widespread use in certain medical treatments. In practice, DMSO is a chemical solvent that is sometimes used to help reduce inflammation and pain, and may also be beneficial in reducing leakage during chemotherapy treatment. Furthermore, DMSO and its oxidative products methylsulfonylmethane (MSM) and dimethyldisulfide (DMS) have been detected in both human cerebrospinal fluid (CSF) or in human plasma, urine, or faeces.<sup>38–40</sup> Although DMSO was reported for the treatment of musculoskeletal conditions, very few peer-reviewed data exist to support claims that DMSO protects or repairs cartilage, or alters the progression of cartilage damage related to KBD or OA.<sup>41</sup> A previous study has found that DMSO is detrimental to cartilage proteoglycan synthesis, and contributes to dehydration of the cartilage and chondrocyte death.<sup>42</sup> In addition, it was found that DMSO concentrations  $\geq 5\%$  suppress equine articular cartilage matrix metabolism.<sup>43</sup> DMSO is enriched in sulphur metabolism; compared with OA, this study also found that sulphur metabolism is an abnormally expressed pathway in KBD. Previous bulk analysis of sulphur in developing chicken cartilage using electron probes showed a significant decrease in the sulphur content of mature cartilage.<sup>44</sup> In a recent study, Zheng et al<sup>45</sup> found that the scores for sulphur metabolism, cysteine metabolism, and disulfidptosis were significantly reduced in OA synovial tissues, suggesting that impaired sulphur metabolism may play a role in OA pathogenesis. In addition, they constructed a sulphur metabolism-associated six-gene signature for OA diagnosis and identified upregulation of the phagocytosis-associated gene, TM9SF2. To date, sulphur metabolism in KBD has not been well studied. Our results provide evidence of the involvement of DMSO and sulphur metabolism in the pathogenesis of KBD and OA, indicating the possible metabolic difference between these two cartilage diseases.

The present study has also revealed that uric acid is differentially expressed in the cartilage of KBD compared to the cartilage of OA. Uric acid is the end product of human purine catabolism, and in the form of soluble serum urate (sUA) has been recognized as a biomarker in diseases such as cardiovascular disease<sup>46</sup> and chronic kidney disease.<sup>47</sup> Gout can be caused by an excessive amount of uric acid in the bloodstream. Specifically, excess uric acid can form solid urate crystals within joints and tissues, which causes inflammation, severe pain, and swelling. Previous evidence suggests that uric acid may participate in OA pathogenesis, and the association between uric acid and OA has long been observed. A previous epidemiology study identified several common risk factors shared by gout and OA, including older age and obesity.<sup>48</sup> These factors contribute to the development and progression of both conditions. Previous studies have implicated synovial fluid urate as a potential OA biomarker, possibly reflecting chondrocyte damage, and people with high uric acid levels

and who are not diagnosed with gout could experience a faster progression of their OA.<sup>48,49</sup> Inflammation is suggested to be a shared pathogenesis pathway between crystal-induced arthritis and OA.<sup>50</sup> Research suggests that individuals with gout have a higher likelihood of being diagnosed with OA compared to those without gout. Furthermore, the severity of OA tends to be greater in patients with gout compared to individuals without gout.<sup>51</sup> According to the current study, levels of uric acid are found to be upregulated in the KBD cartilage compared to the OA cartilage. This suggests that the cartilage damage in KBD may be more severe than that observed in OA cartilage. In addition, urate is the end product of purine metabolism in humans; we also found that purine metabolism contributes to the pathogenesis of OA and KBD. Purines are a class of organic compounds that play crucial roles in various biological processes, which act as the bases of nucleotides to constitute biological genetic material and energy units (adenosine triphosphate). Purine nucleotides are mainly synthesized from pentose phosphates, amino acids, one-carbon units, and carbon dioxide through a series of enzymatic reactions. Once synthesized, purine nucleotides undergo metabolic pathways that eventually lead to their breakdown into uric acid under the action of xanthine oxidase. Purine metabolism consists of de novo synthesis, catabolism, and salvage pathways. Adenosine is a purine nucleoside and is produced by the conversion of intracellular and extracellular adenine nucleotides. A recent study has revealed that a disorder of purine metabolism could be observed in the development of osteoporosis.<sup>52</sup> Chondrocytes and cartilage might be disproportionately affected by endogenous adenosine levels, which play a critical role in endogenous and exogenous treatment and reversal of OA.<sup>53</sup>

Some limitations should be noted in the present study. First, this is an initial screening of potentially involved metabolites in the pathogenesis of KBD and OA. Further validation through subsequent experiments is necessary to confirm these findings. Second, the alterations in metabolites present in the blood, urine, and synovial fluid samples of patients with OA and KBD should be identified and compared with the metabolic findings in cartilage tissue.

In conclusion, in the current study we conducted comprehensive metabolomics profiling in the cartilage of OA and KBD, and compared the differentially expressed metabolites between the two diseases. We identified several important metabolites and pathways involved in the potential mechanisms of cartilage damage of KBD and OA. This finding highlights the distinct pathogenetic mechanisms of cartilage damage underlying these two conditions.

### Supplementary material

Comprehensive details on all first-level and second-level metabolites identified in the study. Additionally, the ion chromatograms of all samples are included, along with the mass-to-charge ratio (m/z) width and retention time width of our mass spectrometry data.

## References

1. Zhang B, Yang L, Wang W, Li Y, Li H. Environmental selenium in the Kashin-Beck disease area, Tibetan Plateau, China. *Environ Geochem Health*. 2011;33(5):495–501.
2. Guo X, Ma W-J, Zhang F, Ren F-L, Qu C-J, Lammi MJ. Recent advances in the research of an endemic osteochondropathy in China: Kashin-Beck disease. *Osteoarthritis Cartilage*. 2014;22(11):1774–1783.
3. Yang HJ, Zhang Y, Wang ZL, et al. Increased chondrocyte apoptosis in Kashin-Beck disease and rats induced by T-2 toxin and selenium deficiency. *Biomed Environ Sci*. 2017;30(5):351–362.
4. Ning Y, Zhang P, Zhang F, et al. Abnormal expression of TSG-6 disturbs extracellular matrix homeostasis in chondrocytes from endemic osteoarthritis. *Front Genet*. 2022;13:1064565.
5. Wang X, Ning Y, Li C, et al. Alterations in the gut microbiota and metabolite profiles of patients with Kashin-Beck disease, an endemic osteoarthritis in China. *Cell Death Dis*. 2021;12(11):1015.
6. Han J, Wang W, Qu C, et al. Role of inflammation in the process of clinical Kashin-Beck disease: latest findings and interpretations. *Inflamm Res*. 2015;64(11):853–860.
7. Shi XW, Guo X, Lv AL, et al. Heritability estimates and linkage analysis of 23 short tandem repeat loci on chromosomes 2, 11, and 12 in an endemic osteochondropathy in China. *Scand J Rheumatol*. 2010;39(3):259–265.
8. Shi XW, Guo X, Ren FL, Li J, Wu XM. The effect of short tandem repeat loci and low selenium levels on endemic osteoarthritis in China. *J Bone Joint Surg Am*. 2010;92-A(1):72–80.
9. Salman LA, Ahmed G, Dakin SG, Kendrick B, Price A. Osteoarthritis: a narrative review of molecular approaches to disease management. *Arthritis Res Ther*. 2023;25(1):27.
10. He C-P, Chen C, Jiang X-C, et al. The role of AGEs in pathogenesis of cartilage destruction in osteoarthritis. *Bone Joint Res*. 2022;11(5):292–300.
11. Yang J, Fan Y, Liu S. ATF3 as a potential diagnostic marker of early-stage osteoarthritis and its correlation with immune infiltration through bioinformatics analysis. *Bone Joint Res*. 2022;11(9):679–689.
12. Sandell LJ. Etiology of osteoarthritis: genetics and synovial joint development. *Nat Rev Rheumatol*. 2012;8(2):77–89.
13. Lian W, Liu H, Song Q, et al. Prevalence of hand osteoarthritis and knee osteoarthritis in Kashin-Beck disease endemic areas and non Kashin-Beck disease endemic areas: a status survey. *PLoS One*. 2018;13(1):e0190505.
14. Yao Q, Wu X, Tao C, et al. Osteoarthritis: pathogenic signaling pathways and therapeutic targets. *Signal Transduct Target Ther*. 2023;8(1):56.
15. Zhang F, Guo X, Duan C, Wu S, Yu H, Lammi M. Identification of differentially expressed genes and pathways between primary osteoarthritis and endemic osteoarthritis (Kashin-Beck disease). *Scand J Rheumatol*. 2013;42(1):71–79.
16. Ning Y, Hu M, Gong Y, et al. Comparative analysis of the gut microbiota composition between knee osteoarthritis and Kashin-Beck disease in Northwest China. *Arthritis Res Ther*. 2022;24(1):129.
17. Johnson CH, Ivanisevic J, Siuzdak G. Metabolomics: beyond biomarkers and towards mechanisms. *Nat Rev Mol Cell Biol*. 2016;17(7):451–459.
18. Wang YM, Wang WY, Sun LY, et al. Serum metabolomic indicates potential biomarkers and metabolic pathways of pediatric Kashin-Beck disease. *Biomed Environ Sci*. 2020;33(10):750–759.
19. Wu X, Liyanage C, Plan M, et al. Dysregulated energy metabolism impairs chondrocyte function in osteoarthritis. *Osteoarthritis Cartilage*. 2023;31(5):613–626.
20. Mobasheri A, Rayman MP, Gualillo O, Sellam J, van der Kraan P, Fearon U. The role of metabolism in the pathogenesis of osteoarthritis. *Nat Rev Rheumatol*. 2017;13(5):302–311.
21. Akhbari P, Karamchandani U, Jaggard MKJ, et al. Can joint fluid metabolic profiling (or “metabonomics”) reveal biomarkers for osteoarthritis and inflammatory joint disease?: A systematic review. *Bone Joint Res*. 2020;9(3):108–119.
22. Samuel AJ, Kanimozhi D. Outcome measures used in patient with knee osteoarthritis: With special importance on functional outcome measures. *Int J Health Sci (Qassim)*. 2019;13(1):52–60.
23. Wang X, Ning Y, Zhang P, et al. Comparison of the major cell populations among osteoarthritis, Kashin-Beck disease and healthy chondrocytes by single-cell RNA-seq analysis. *Cell Death Dis*. 2021;12(6):551.
24. Yu C, Luo X, Zhan X, et al. Comparative metabolomics reveals the metabolic variations between two endangered *Taxus* species (*T. fuana* and *T. yunnanensis*) in the Himalayas. *BMC Plant Biol*. 2018;18(1):197.
25. Li Y, Fang J, Qi X, et al. Combined analysis of the fruit metabolome and transcriptome reveals candidate genes involved in flavonoid biosynthesis in *Actinidia arguta*. *Int J Mol Sci*. 2018;19(5):1471.
26. Hou Y, Tan E, Shi H, et al. Mitochondrial oxidative damage reprograms lipid metabolism of renal tubular epithelial cells in the diabetic kidney. *Cell Mol Life Sci*. 2024;81(1):23.
27. Smith CA, Want EJ, O’Maille G, Abagyan R, Siuzdak G. XCMS: processing mass spectrometry data for metabolite profiling using nonlinear peak alignment, matching, and identification. *Anal Chem*. 2006;78(3):779–787.
28. Kuhl C, Tautenhahn R, Böttcher C, Larson TR, Neumann S. CAMERA: an integrated strategy for compound spectra extraction and annotation of liquid chromatography/mass spectrometry data sets. *Anal Chem*. 2012;84(1):283–289.
29. Wen B, Mei Z, Zeng C, Liu S. metaX: a flexible and comprehensive software for processing metabolomics data. *BMC Bioinformatics*. 2017;18(1):183.
30. Kanehisa M, Goto S. KEGG: kyoto encyclopedia of genes and genomes. *Nucleic Acids Res*. 2000;28(1):27–30.
31. Ning Y, Chen S, Zhang F, et al. The alteration of urinary metabolomics profiles in Kashin-Beck disease in a three consecutive year study. *Mol Omics*. 2023;19(2):137–149.
32. Wu C, Lei R, Tiainen M, et al. Disordered glycometabolism involved in pathogenesis of Kashin-Beck disease, an endemic osteoarthritis in China. *Exp Cell Res*. 2014;326(2):240–250.
33. Cao J, Li S, Shi Z, et al. Articular cartilage metabolism in patients with Kashin-Beck Disease: an endemic osteoarthropathy in China. *Osteoarthritis Cartilage*. 2008;16(6):680–688.
34. Kang D, Lee J, Wu C, et al. The role of selenium metabolism and selenoproteins in cartilage homeostasis and arthropathies. *Exp Mol Med*. 2020;52(8):1198–1208.
35. Su Z, Zong Z, Deng J, et al. Lipid metabolism in cartilage development, degeneration, and regeneration. *Nutrients*. 2022;14(19):3984.
36. Abshirini M, Ilesanmi-Oyelere BL, Kruger MC. Potential modulatory mechanisms of action by long-chain polyunsaturated fatty acids on bone cell and chondrocyte metabolism. *Prog Lipid Res*. 2021;83:101113.
37. Liu L, Zhang W, Liu T, et al. The physiological metabolite  $\alpha$ -ketoglutarate ameliorates osteoarthritis by regulating mitophagy and oxidative stress. *Redox Biol*. 2023;62:102663.
38. Williams KI, Burstein SH, Layne DS. Dimethyl sulfone: isolation from human urine. *Arch Biochem Biophys*. 1966;113(1):251–252.
39. Engelke UFH, Tangerman A, Willemsen MAAP, et al. Dimethyl sulfone in human cerebrospinal fluid and blood plasma confirmed by one-dimensional (1)H and two-dimensional (1)H-(13)C NMR. *NMR Biomed*. 2005;18(5):331–336.
40. Garner CE, Smith S, de Lacy Costello B, et al. Volatile organic compounds from feces and their potential for diagnosis of gastrointestinal disease. *FASEB J*. 2007;21(8):1675–1688.
41. Yang C, Madhu V, Thomas C, et al. Inhibition of differentiation and function of osteoclasts by dimethyl sulfoxide (DMSO). *Cell Tissue Res*. 2015;362(3):577–585.
42. Matthews GL, Engler SJ, Morris EA. Effect of dimethylsulfoxide on articular cartilage proteoglycan synthesis and degradation, chondrocyte viability, and matrix water content. *Vet Surg*. 1998;27(5):438–444.
43. Smith CL, MacDonald MH, Tesch AM, Willits NH. In vitro evaluation of the effect of dimethyl sulfoxide on equine articular cartilage matrix metabolism. *Vet Surg*. 2000;29(4):347–357.
44. Hargest TE, Gay CV, Schraer H, Wasserman AJ. Vertical distribution of elements in cells and matrix of epiphyseal growth plate cartilage determined by quantitative electron probe analysis. *J Histochem Cytochem*. 1985;33(4):275–286.
45. Zheng S, Li Y, Yin L, Lu M. Identification of sulfur metabolism-related gene signature in osteoarthritis and TM9SF2’s sustenance effect on M2 macrophages’ phagocytic activity. *J Orthop Surg Res*. 2024;19(1):62.
46. Li X, Meng X, He Y, et al. Genetically determined serum urate levels and cardiovascular and other diseases in UK Biobank cohort: a phenome-wide mendelian randomization study. *PLoS Med*. 2019;16(10):e1002937.
47. Weaver DJ. Uric acid and progression of chronic kidney disease. *Pediatr Nephrol*. 2019;34(5):801–809.

48. Yokose C, Chen M, Berhanu A, Pillinger MH, Krasnokutsky S. Gout and osteoarthritis: associations, pathophysiology, and therapeutic implications. *Curr Rheumatol Rep*. 2016;18(10):65.
49. Krasnokutsky S, Oshinsky C, Attur M, et al. Serum urate levels predict joint space narrowing in non-gout patients with medial knee osteoarthritis. *Arthritis Rheumatol*. 2017;69(6):1213–1220.
50. Ma CA, Leung YY. Exploring the link between uric acid and osteoarthritis. *Front Med (Lausanne)*. 2017;4:225.
51. Howard RG, Samuels J, Gyftopoulos S, et al. Presence of gout is associated with increased prevalence and severity of knee osteoarthritis among older men: results of a pilot study. *J Clin Rheumatol*. 2015;21(2):63–71.
52. Yang K, Li J, Tao L. Purine metabolism in the development of osteoporosis. *Biomed Pharmacother*. 2022;155:113784.
53. Cronstein BN, Angle SR. Purines and adenosine receptors in osteoarthritis. *Biomolecules*. 2023;13(12):1760.

### Author information

H. Chang, MSc, Attending Physician  
Q. Zhang, BSc, Chief Physician  
G. Xu, BSc, Attending Physician  
P. Chen, BSc, Chief Physician  
C. Li, BSc, Attending Physician  
X. Guo, MSc, Associate Chief Physician  
Z. Yang, BSc, Associate Chief Physician  
Shaanxi Provincial Institute for Endemic Disease Control, Xi'an, China.

L. Liu, PhD candidate  
F. Zhang, PhD, Professor  
School of Public Health, Health Science Center, Xi'an Jiaotong University, Xi'an, China.

J. Wang, MD, Physician, Department of Joint Surgery, Honghui Hospital, Xi'an Jiaotong University, Xi'an, China.

### Author contributions

H. Chang: Conceptualization, Writing – original draft.  
L. Liu: Formal analysis, Investigation, Writing – original draft.  
Q. Zhang: Investigation, Writing – review & editing.  
G. Xu: Investigation, Writing – review & editing.  
J. Wang: Investigation, Writing – review & editing.  
P. Chen: Formal analysis, Writing – review & editing.  
C. Li: Validation, Writing – review & editing.  
X. Guo: Investigation, Writing – review & editing.  
Z. Yang: Conceptualization, Resources, Writing – review & editing.  
F. Zhang: Conceptualization, Funding acquisition.

H. Chang and L. Liu contributed equally to this work.

### Funding statement

The authors disclose receipt of the following financial or material support for the research, authorship, and/or publication of this article: this work was supported by the National Natural Scientific Foundation of China (81922059) and the Natural Science Basic

Research Plan in Shaanxi Province of China (2021JCW-08), as reported by F. Zhang.

### ICMJE COI statement

F. Zhang reports grants from the National Natural Scientific Foundation of China (81922059) and the Natural Science Basic Research Plan in Shaanxi Province of China (2021JCW-08), related to this study.

### Data sharing

The data for this study will be publicly available (from 14 March 2025) at: [www.ebi.ac.uk/metabolights/MTBLS9743](http://www.ebi.ac.uk/metabolights/MTBLS9743).

### Acknowledgements

We are grateful to the patients, orthopaedic surgeons, and nurses at the Red Cross Hospital of Xi'an Jiaotong University for providing the clinical materials.

### Ethical review statement

The study was approved by the Ethical Committee of Xi'an Jiaotong University (No. 685). All the participants gave their informed consent by signing a document that the Ethical Committee of Xi'an Jiaotong University had carefully reviewed.

### Open access funding

The authors report that the open access funding for their manuscript was self-funded.

© 2024 Chang et al. This is an open-access article distributed under the terms of the Creative Commons Attribution Non-Commercial No Derivatives (CC BY-NC-ND 4.0) licence, which permits the copying and redistribution of the work only, and provided the original author and source are credited. See <https://creativecommons.org/licenses/by-nc-nd/4.0/>